Frequency-addressed tunable transmission in optically thin metallic nanohole arrays with dual-frequency liquid crystals

Qingzhen Hao,[1,2] Yanhui Zhao,[1] Bala Krishna Juluri,[1] Brian Kiraly,[1] Justin Liou,[3] Iam Choon Khoo,[3] and Tony Jun Huang[1,a)]
[1]*Department of Engineering Science and Mechanics, The Pennsylvania State University, University Park, Pennsylvania 16802, USA*
[2]*Department of Physics, The Pennsylvania State University, University Park, Pennsylvania 16802, USA*
[3]*Department of Electrical Engineering, The Pennsylvania State University, University Park, Pennsylvania 16802, USA*

(Received 18 October 2010; accepted 22 March 2011; published online 27 April 2011)

Frequency-addressed tunable transmission is demonstrated in optically thin metallic nanohole arrays embedded in dual-frequency liquid crystals (DFLCs). The optical properties of the composite system are characterized by the transmission spectra of the nanoholes, and a prominent transmission peak is shown to originate from the resonance of localized surface plasmons at the edges of the nanoholes. An ~17 nm shift in the transmission peak is observed between the two alignment configurations of the liquid crystals. This DFLC-based active plasmonic system demonstrates excellent frequency-dependent switching behavior and could be useful in future nanophotonic applications. © *2011 American Institute of Physics*. [doi:10.1063/1.3581037]

I. INTRODUCTION

Since Ebbesen et al. reported extraordinary optical transmission through two-dimensional arrays of sub-wavelength holes in perforated silver films,[1] there has been a tremendous surge in investigations into surface plasmons (SPs).[2–4] The photon-electron interactions at these nanostructures allow the confinement of electromagnetic waves to nanoscale dimensions with strong field localization and enhancement.[5] These properties enable nanohole arrays in metal films to have many applications, including optical switching, color filtering, polarization control, nanolithography, sub-diffraction imaging, sensing, and enhanced spectroscopy.[5–10] Similar to their nanoparticle counterparts, resonances from nanoholes in perforated optically thin metallic films are sensitive to the shape, size, and spacing of the structures.[11–17] Additionally, the dielectric constant of the surrounding medium plays an important role in the resonances.[18] This dependence can be exploited with the use of active materials in the surroundings, which could provide the ability to affect dynamic, continuous, and reversible changes in the plasmonic resonances for "active plasmonics."[8,19–25]

In this article, we demonstrate a frequency-addressed active plasmonic system based on the transmission of a uniform nanohole array perforated in an optically thin Au film covered by nematic dual-frequency liquid crystals (DFLCs). By applying an electric field alternating at low and high frequencies, it is possible to switch the DFLC director (the long axis of the rod-like liquid crystal molecules) in directions both parallel and perpendicular to the field,[26,27] thus reversibly changing their dielectric anisotropy from positive to negative. The changes in the alignment configuration of DFLCs lead directly to sizable shifts in the plasmonic resonances, thereby giving controllable transmission through the nanoholes.

II. EXPERIMENT AND DISCUSSION

The experimental setup is shown in Fig. 1(a). A highly ordered nanohole array in a 30 nm gold film is fabricated by e-beam lithography.[28] The perforated film is transferred to a clean indium tin oxide (ITO) coated glass slide. A monolayer of hexadecyl trimethyl ammonium bromide (HTAB) is self-assembled on a bare ITO glass and the nanohole substrate to achieve homeotropic alignment of the DFLCs (i.e., DFLCs align perpendicular to the substrate).[29] The two slides, serving as electrodes, are brought together to form a liquid crystal (LC) cell. The cell thickness, ~5 μm, is defined by polystyrene microbead spacers. All of the experimental measurements are done at room temperature, ~21 °C. The DFLCs used are MLC-2048 (Merck), which have a positive dielectric anisotropy, $\Delta\varepsilon > 0$ (where $\Delta\varepsilon = \varepsilon_{//} - \varepsilon_{\perp}$) for frequencies, f, less than the crossover frequency, $f_c \sim 12$ kHz (at 20 °C), and a negative anisotropy when $f > f_c$.[30] Here $\varepsilon_{//}$ and $\varepsilon_{\perp}$ are the dielectric permittivities of the DFLCs parallel and perpendicular to the LC director, respectively. For DFLCs with $\Delta\varepsilon > 0$, the director prefers to align with the electric field while for $\Delta\varepsilon < 0$, it aligns perpendicular to the electric field [Fig. 1(b)]. The DFLCs used here have an ordinary refractive index, $n_o = 1.4978$, and an optical birefringence, $\Delta n = 0.2214$ at $\lambda = 589$ nm (i.e., an extraordinary refractive index, $n_e = 1.7192$).

A field emission scanning electron microscope (FE-SEM) image of the fabricated nanohole array is shown in Fig. 1(c); the array has an average period of ~300 nm in a square lattice with a hole diameter of ~120 nm. Transmission spectra of the sample were collected with an unpolarized white-light beam (HR4000CG-UV-NIR, Ocean Optics). As shown in Fig. 1(d), for bare Au nanoholes in air, the main transmission peak

a)Author to whom correspondence should be addressed. Electronic mail: junhuang@psu.edu.

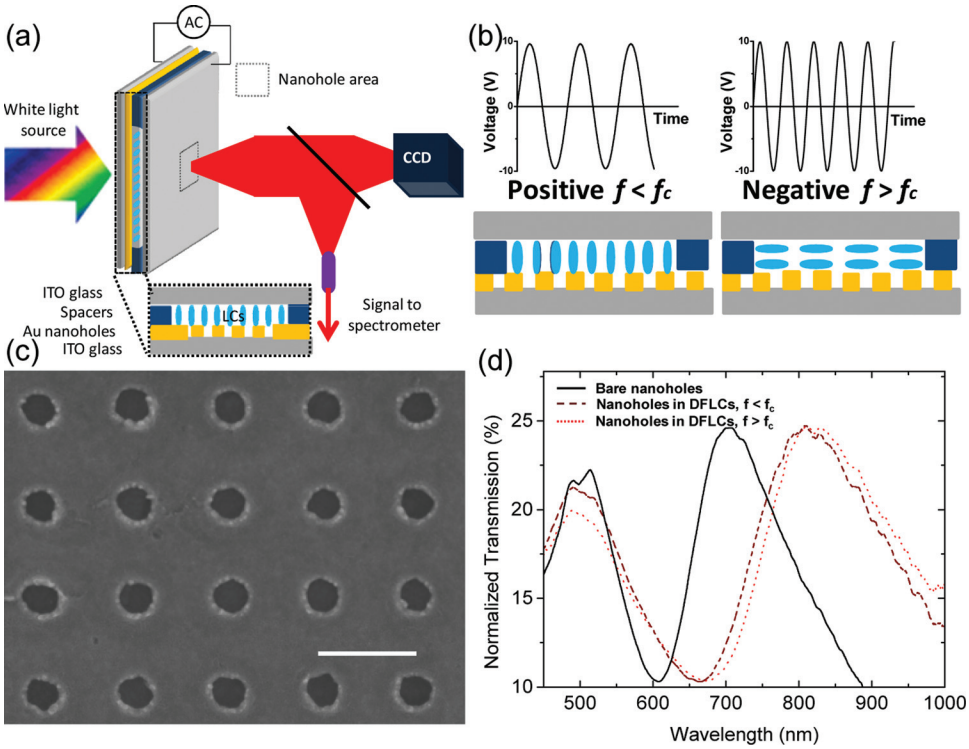

FIG. 1. (Color online) (a) Schematic showing the experimental setup. (b) Schematic depicting the orientation of DFLCs for voltage with different frequencies. (c) FE-SEM image of the Au nanohole array. (d) Transmission spectra of the nanohole array in three different environments.

appears at $\lambda = 700$ nm; after the injection of LCs in homeotropic alignment, the transmission peak red-shifts to 804 nm. A high-frequency ($f > f_c$) electric field aligns the LCs parallel to the substrate causing the transmission peak to further shift to 821 nm. The transmission spectra are normalized to visualize changes in the peak position, and the dependence of transmission on voltage and frequency are studied below in detail.

Figure 2(a) shows the voltage-dependent transmission spectra when the frequency is fixed at 1 kHz ($f = 1$ kHz $< f_c$). In this case, $\Delta\varepsilon > 0$, and the LCs retain their homeotropic alignment. Regardless of the polarization, the probe light only encounters the ordinary refractive index of the DFLCs resulting in little change in the transmission as the applied voltage is increased. At a high frequency ($f = 25$ kHz $> f_c$), the liquid crystal exhibits a negative dielectric anisotropy, $\Delta\varepsilon < 0$. However, the LC molecules start to switch into horizontal alignment only when the applied voltage exceeds an ~16 V threshold. Here the threshold refers to the voltage that induces the reorientation of the LC molecular layer that is in the vicinity (~100 nm) of Au nanoholes.[31] Since we did not impart a preferred direction for the director axis in the plane of the substrate, the probe light sees a combination of the ordinary refraction index (n_o) and the extraordinary refractive index (n_e). For the unpolarized probe light used in our experiment, the effective refractive index at a high-frequency voltage can be estimated as $n_{ef} \cong \sqrt{(n_o^2 + n_e^2)/2} = 1.6123$, which is larger than that of the LCs in homeotropic alignment. Therefore, after the LC realignment, the transmission decreases and its peak red-shifts to ~821 nm, as illustrated in Fig. 2(b). A larger voltage induces a higher percentage of the LC realignment and results in a further decrease in the observed transmission.

Since the dielectric anisotropy of the DFLCs is strongly dependent on the frequency, we can tune the transmission of the nanohole array by varying the frequency of the applied field. Figure 3 shows the transmission spectra of the nanoholes for different frequencies with a fixed amplitude of 20 V. The initially observed crossover frequency is ~15 kHz, and when

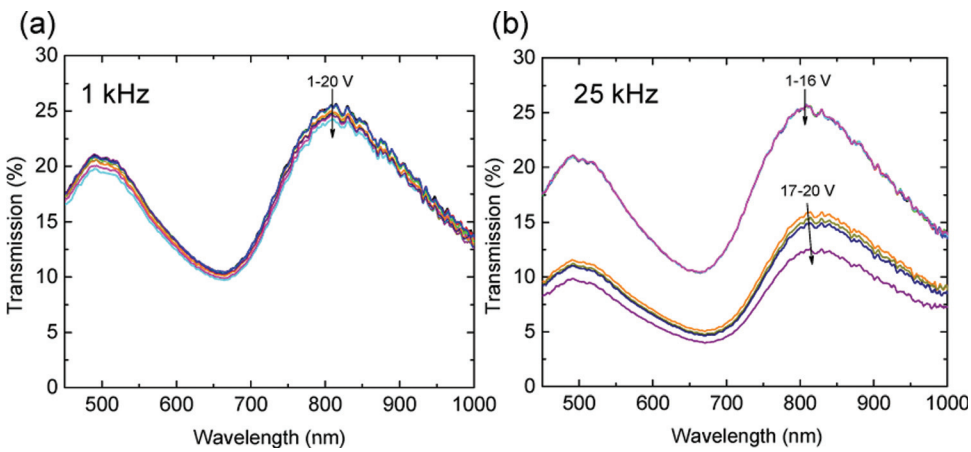

FIG. 2. (Color online) Voltage-dependent transmission spectra of the nanohole array with the frequency fixed at (a) 1 kHz and (b) 25 kHz. The voltages have even increments.

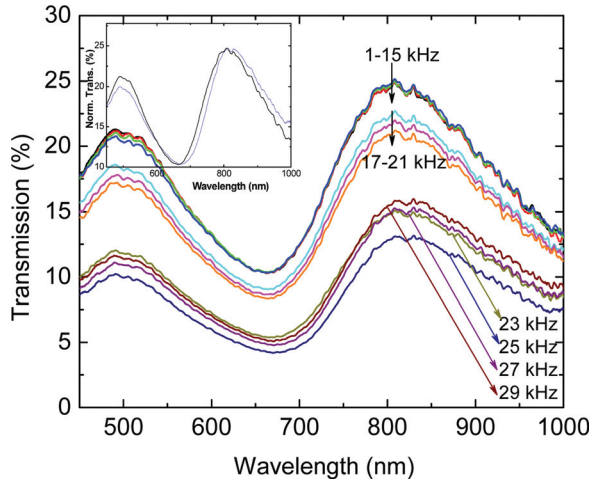

FIG. 3. (Color online) Frequency-dependent transmission spectra of the nanohole array with voltage fixed at $V = 20$ V. Inset shows the normalized spectra for 1 and 25 kHz. The voltages have even increments.

the frequency of the applied field is below this threshold, the transmission peak remains unchanged except for minor fluctuations in intensity. However, Wen *et al*. have shown that the crossover frequency of MLC-2048 increases exponentially with the temperature.[32] The applied high-frequency electric field generates heat, which in turn shifts the crossover frequency to ~23 kHz. For frequencies above 23 kHz, the LC molecules realign parallel to the substrate, causing the probe light to see an increased refractive index, resulting in decreases in the transmission and shifts in the peak position. The transmission is minimized at a frequency of 25 kHz, with the transmission peak red-shifting to ~821 nm. Figure 2(b) is consistent with Fig. 3 which shows excellent reproducibility. In both cases, we observe a ~17 nm red-shift in the transmission peak between the two alignment configurations of the LCs.

Previous studies on metallic nanoparticles have shown that their localized surface plasmon resonance (LSPR) peak shifts linearly with the surrounding refractive index.[33,34] The transmission peak observed in the nanoholes is analogous to LSPR in nanoparticles, and we therefore expect the transmission of the nanoholes to have a similar dependence on the surrounding refractive index. By comparing transmission peaks before and after injection of the LCs we estimate that the sensitivity factor for the nanoholes is approximately 209 nm per refractive index unit. For the DFLCs used in this experiment ($n_{\text{eff}} = 1.6123$) an ~0.11 refractive index unit increase from the perfect homeotropic state ($n_0 = 1.4978$) is predicted to induce an ~23 nm red-shift in the nanohole LSPR. This result agrees reasonably well with our measurement. A smaller observed shift most likely indicates that the LCs near the nanoholes cannot completely realign. It is worth noting that above 25 kHz, the DFLCs start to exhibit a multi-domain state which strongly scatters the probe light, leading to a slight increase in the transmission intensity. The multi-domain state, however, does not affect the reversibility and reproducibility of the transmission peak shift, fulfilling an important requirement for an active plasmonic device.

Finite-difference time-domain (FDTD) (Lumerical)[35] techniques were used to predict the changes in the transmission of the nanoholes. A square nanohole array with a lattice constant of 300 nm in a 30 nm thick Au film was simulated with periodic boundary conditions. The dielectric function built into the software was used for the metal.[36] The simulated transmission spectrum of the bare Au nanohole array is shown in Fig. 4(a). The simulation agrees well with the experiments [Fig. 1(d)] with one exception: a small peak at ~580 nm in the simulation. The existence of the peak can be explained by the presence of propagating surface plasmon polaritons (SPPs). It is well known that periodic arrays can provide the additional momentum required to couple incoming light to SPPs; in nanohole arrays this leads to a transmission peak at $\lambda_{\max} = (a/\sqrt{i^2 + j^2})\sqrt{\varepsilon_D \varepsilon_M/(\varepsilon_D + \varepsilon_M)}$,where ε_M and ε_D are the dielectric function of the metal and the dielectric, respectively, a is the lattice constant of the array, and i and j are integers.[37] In our case, the small peak at ~580 nm in the simulation (it is experimentally difficult to pick up a peak with such small intensity) indeed satisfies the above expression for a (1, 0) mode at an air/Au interface. The main peak at $\lambda = 700$ nm, however, entirely deviates from this $\lambda_{\max}$, indicating that it does not originate from the SPPs; instead, the simulated electric field distribution [Fig. 4(b)] reveals that this transmission peak originates from the resonance of localized SPs near the edges of the holes: the strong field is localized near the hole edges rather than on the film between the holes. Unlike SPPs in optically thick films, localized SP charges oscillate and act as dipolar antenna in our optically thin film to directly radiate light into the far field.[28,38] Localized SPs are dipolar in nature, and therefore have properties similar to LSPRs in nanoparticles. The simulations were further used to confirm the transmission changes introduced by the two different LC

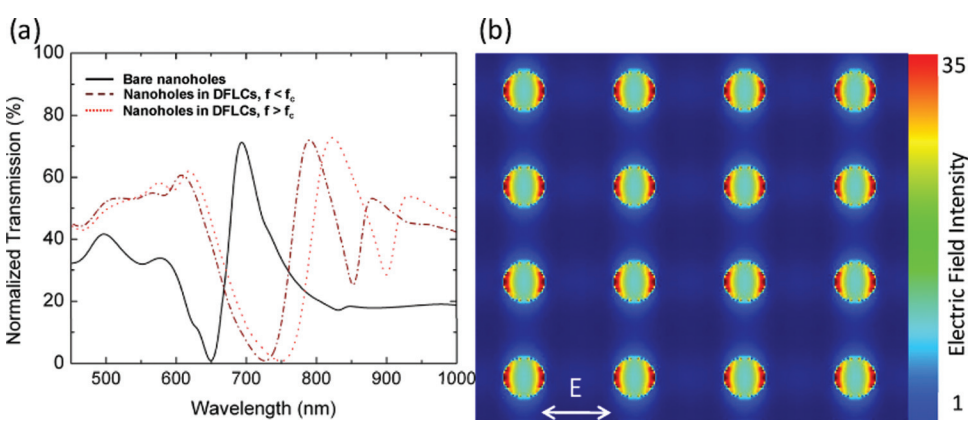

FIG. 4. (Color online) (a) FDTD simulation of the transmission of the nanohole arrays in the three environments. (b) Simulated electric field intensity distribution at the resonance (700 nm) of the nanohole array.

orientations: perpendicular to the substrate ($f < f_c$) and parallel to the substrate ($f > f_c$). The simulations modeled nanoholes embedded in a ~100 nm thick effective medium with $n_o = 1.4978$ and $n_{ef} = 1.6123$. As expected, the transmission peak shifts from ~800 to ~826 nm between the two LC orientations, which agrees reasonably well with the experimental results. The broader experimental resonances are likely caused by larger losses in the thin film (electrons suffer more scattering at the surface of the optical thin film) and nonuniformities of the sample (i.e., inhomogeneous broadening).

III. CONCLUSION

In conclusion, we have demonstrated frequency-addressed tunable transmission in a uniform Au nanohole array embedded in DFLCs. The frequency-dependent dielectric properties of the DFLCs induce a shift of the transmission peak. This mechanism enables us to actively control the spectral location of the transmission peak by manipulating the alignment of the DFLCs. We are currently exploring the tunability of the LC director axis with optical fields, which could give rise to extremely fast response speeds in the sub-microsecond regime[39,40] and would not require the imposition of electrodes. This DFLC-based active plasmonic system demonstrates excellent frequency-dependent switching behavior, and can potentially be used in active polarizers and filters, chip-based optical communications, and nanoplasmonic circuits.

ACKNOWLEDGMENTS

We gratefully acknowledge the financial support from Air Force Office of Scientific Research (AFOSR), National Science Foundation (NSF), and the Penn State Center for Nanoscale Science (MRSEC). Components of this work were conducted at the Penn State node of the NSF-funded National Nanotechnology Infrastructure Network (NNIN).

[1]T. W. Ebbesen, H. J. Lezec, H. F. Ghaemi, T. Thio, and P. A. Wolff, Nature (London) **391**, 667 (1998).
[2]W. L. Barnes, A. Dereux, and T. W. Ebbesen, Nature (London) **424**, 824 (2003).
[3]N. Fang, H. Lee, C. Sun, and X. Zhang, Science **308**, 534 (2005).
[4]Y. Alaverdyan, B. Sepulveda, L. Eurenius, E. Olsson, and M. Kall, Nat. Phys. **3**, 884 (2007).
[5]C. Genet and T. W. Ebbesen, Nature (London) **445**, 39 (2007).
[6]R. Gordon, A. G. Brolo, D. Sinton, and K. L. Kavanagh, Laser Photonics Rev. **4**, 311 (2010).
[7]Z. W. Liu, Y. Wang, J. Yao, H. Lee, W. Srituravanich, and X. Zhang, Nano Lett. **9**, 462 (2009).
[8]D. K. Gramotnev and S. I. Bozhevolnyi, Nat. Photonics **4**, 83 (2010).
[9]E. Ozbay, Science **311**, 189 (2006).
[10]Q. Hao, B. K. Juluri, Y. B. Zheng, B. Wang, I. Chiang, L. Jensen, V. Crespi, P.C. Eklund, and T. J. Huang, J. Phys. Chem. C **114**, 18059 (2010).
[11]F. J. G. de Abajo, Rev. Mod. Phys. **79**, 1267 (2007).
[12]B. Sepulveda, Y. Alaverdyan, J. Alegret, M. Kall, and P. Johansson, Opt. Express **16**, 5609 (2008).
[13]T. H. Park, N. Mirin, J. B. Lassiter, C. L. Nehl, N. J. Halas, and P. Nordlander, ACS Nano **2**, 25 (2008).
[14]Y. Gu, J. Li, O. J. F. Martin, and Q. H. Gong, J. Appl. Phys. **107**, 114313 (2010).
[15]Y. B. Zheng, B. K. Juluri, L. L. Jensen, D. Ahmed, M. Lu, L. Jensen, and T. J. Huang, Adv. Mater. **22**, 3603 (2010).
[16]Y. B. Zheng, L. L. Jensen, W. Yan, T. R. Walker, B. K. Juluri, L. Jensen, and T. J. Huang, J. Phys. Chem. C **113**,7019 (2009).
[17]Y. Zheng, T. J. Huang, A. Y. Desai, S. J. Wang, L. K. Tan, H. Gao, and A. C. H. Huan, Appl. Phys. Lett. **90**, 183117 (2007).
[18]J. Henzie, J. Lee, M. H. Lee, W. Hasan, and T. W. Odom, Annu. Rev. Phys. Chem. **60**, 147 (2009).
[19]V. K. S. Hsiao, Y. B. Zheng, B. K. Juluri, and T. J. Huang, Adv. Mater. **20**, 3528 (2008).
[20]Y. J. Liu, Q. Z. Hao, J. S. T. Smalley, J. Liou, I. C. Khoo, and T. J. Huang, Appl. Phys. Lett. **97**, 091101 (2010).
[21]D. P. Gaillot, E. Graugnard, J. S. King, and C. J. Summers, J. Opt. Soc. Am. B **24**, 990 (2007).
[22]A. Minovich, D. N. Neshev, D. A. Powell, I. V. Shadrivov, and Y. S. Kivshar, Appl. Phys. Lett. **96**, 193103 (2010).
[23]A. V. Krasavin and N. I. Zheludev, Appl. Phys. Lett. **84**, 1416 (2004).
[24]V. V. Temnov, G. Armelles, U. Woggon, D. Guzatov, A. Cebollada, A. Garcia-Martin, J. M. Garcia-Martin, T. Thomay, A. Leitenstorfer, and R. Bratschitsch, Nat. Photonics **4**, 107 (2010).
[25]Y. B. Zheng, Y. W. Yang, L. Jensen, L. Fang, B. K. Juluri, A. H. Flood, P. S. Weiss, J. F. Stoddart, and T. J. Huang, Nano Lett. **9**, 819 (2009).
[26]Y. H. Fan, H. W. Ren, X. Liang, Y. H. Lin, and S. T. Wu, Appl. Phys. Lett. **85**, 2451 (2004).
[27]E. Graugnard, J. S. King, S. Jain, C. J. Summers, Y. Zhang-Williams, and I. C. Khoo, Phys. Rev. B **72**, 233105 (2005).
[28]Q. Hao, Y. Zeng, X. Wang, Y. Zhao, B. Wang, I. Chiang, D. H. Werner, V. Crespi, and T. J. Huang, Appl. Phys. Lett. **97**, 193101 (2010).
[29]A. Petrossian and S. Residori, Europhys. Lett. **60**, 79 (2002).
[30]O. Pishnyak, S. Sato, and O. D. Lavrentovich, Appl. Optics **45**, 4576 (2006).
[31]A. J. Haes, C. L. Haynes, A. D. McFarland, G. C. Schatz, R. R. Van Duyne, and S. L. Zou, MRS Bull. **30**, 368 (2005).
[32]C. H. Wen and S. T. Wu, Appl. Phys. Lett. **86**, 231104 (2005).
[33]A. D. McFarland and R. P. Van Duyne, Nano Lett. **3**, 1057 (2003).
[34]Y. B. Zheng, B. K. Juluri, X. L. Mao, T. R. Walker, and T. J. Huang, J. Appl. Phys. **103**, 014308 (2008).
[35]http://www.lumerical.com.
[36]Marvin J. Weber, *Handbook of Optical Materials* (CRC, Boca Raton, 2002).
[37]S. H. Chang, S. K. Gray, and G. C. Schatz, Opt. Express **13**, 3150 (2005).
[38]Z. J. Zhang, R. W. Peng, Z. Wang, F. Gao, X. R. Huang, W. H. Sun, Q. J. Wang, and M. U. Wang, Appl. Phy. Lett. **93**, 171110 (2008).
[39]I. C. Khoo, Phys. Rep. **471**, 221 (2009).
[40]I. C. Khoo, A. Diaz, J. Liou, M. V. Stinger, J. Huang and Y. Ma, IEEE J. Sel. Top. Quantum Electron. **16**, 410 (2010).